Journal of ELECTRONIC MATERIALS, Vol. 41, No. 6, 2012
DOI: 10.1007/s11664-012-2076-8

Feasibility Study on the Use of a Solar Thermoelectric Cogenerator Comprising a Thermoelectric Module and Evacuated Tubular Collector with Parabolic Trough Concentrator

L. MIAO,[1,4] M. ZHANG,[1] S. TANEMURA,[1,2] T. TANAKA,[3] Y.P. KANG,[1] and G. XU[1]

1.—Key Laboratory for Renewable Energy and Gas Hydrates, Guangzhou Institute of Energy Conversion, Chinese Academy of Sciences, No. 2 Nengyuan Road, Tianhe District, Guangzhou 510640, People's Republic of China. 2.—Material Research & Engineering Lab, Japan Fine Ceramics Center, 2-4-1 Mutsuno, Atsuta-ku, Nagoya 456-8587, Japan. 3.—Tanaka Engineering Consultant Co., Chu-Ou 4-13-8, Ushiku, Ibaraki 300-1234, Japan. 4.—e-mail: miaolei@ms.giec.ac.cn

We have designed a new solar thermoelectric cogeneration system consisting of an evacuated tubular solar collector (ETSC) with a parabolic trough concentrator (PTC) and thermoelectric modules (TEMs) to supply both thermal energy and electricity. The main design concepts are (1) the hot side of the TEM is bonded to the solar selective absorber installed in an evacuated glass tube, (2) the cold side of the TEM is also bonded to the heat sink, and (3) the outer circulated water is heated by residual solar energy after TEM generation. We present an example solar thermal simulation based on energy balance and heat transfer as used in solar engineering to predict the electrical conversion efficiency and solar thermal conversion efficiency for different values of parameters such as the solar insolation, concentration ratio, and TEM *ZT* values.

Key words: Thermoelectric conversion, solar thermoelectric generator, solar cogeneration, evacuated tubular solar collector (ETSC), parabolic trough concentrator (PTC)

INTRODUCTION

Development of alternative and efficient energy technologies to reduce recent increases in energy consumption that contribute to global warming has become an important issue for every country. After the Fukushima disaster in Japan in 2011, the danger of relying on large-scale nuclear power stations has been recognized by the public. Solar energy is the largest and most widely distributed renewable energy resource in the world, representing an attractive alternative. Solar thermal power generation (STPG) and photovoltaic (PV) power generation are currently the two main ways of solar power generation. In comparison with PV systems, the advantages of STPG can be summarized as: feasibility of constructing large-scale systems with outputs in excess of the megawatt (MW) range, low cost, utilization of a wide range of the solar radiation spectrum, and durability against damage during high-temperature operation under intense radiation and in severe temperature environments. On the other hand, disadvantages include the requirement for huge heat transfer/removable systems such as large molten-salt storage tanks, plumbing and pumping components for circulation of the fluid heat-transfer medium, auxiliary heating boiler coupled with a gas turbine, etc., which usually require costly maintenance during long-term operation. One alternative technology is thermoelectric (TE) power generation based on the Seebeck

(Received July 17, 2011; accepted March 20, 2012; published online April 13, 2012)

effect, in which two different metallic or semiconducting (both *n*-type and *p*-type) materials are bonded together and connected to make a closed circuit. When a temperature difference is applied between the two terminals, a thermoelectric voltage is generated. This technology is attractive from two points of view: (a) the ability to convert energy from high entropy to low entropy, and (b) the possibility of combining various waste heat sources with that from solar. Furthermore, a power generation system utilizing a TE module reduces the expensive maintenance costs, because no moving parts are involved and thermal deterioration of the system should not occur.

Telkes[1] studied the physical characteristics of the first solar thermoelectric generator (STEG) in 1954 by collecting thermal energy using a flat-plate glazed solar collector without a concentrator or vacuum. Due to the unattractive performance of the system, however, until recently the concept was abandoned for a long time except for specialist applications such as the autonomous STEGs used in deep-space missions by the National Aeronautics and Space Administration (NASA) during the 1970s and 1980s, and in remote-area telecommunication stations. Since then, significant progress has been made in improving thermoelectric conversion efficiencies[2–4] thanks to progress in materials science, particularly in the area of low-dimensional nanostructures. However, the application of thermoelectric materials in large-scale renewable energy conversion has not yet succeeded.[5] Conventional wisdom is that thermoelectrics are most suitable for waste heat recovery and that materials with significantly higher figures of merit, ZT, are needed for commercialized production.[6–8] Kraemer et al.[9] demonstrated that STEG is an attractive alternative for converting solar energy into electricity by the integration of a high-performance nanostructured TEM with a solar selective absorber (SSA) plate backed with thick thermal insulation in an evacuated vessel, achieving peak efficiency of 4.6% under solar insolation of 1000 W/m^2. The results show that STEG is feasible as a competitive technology to STPG and PV generation, requiring only modest further improvements to be attained.[10] Motivated by this promising new approach, a recent theoretical calculation of STEG in combination with a concentrator showed that the maximum efficiency exceeds 10% in a system with a geometric optical concentration ratio of 45 (a value obtainable with a *p*–*n* junction of skutterudite and bismuth telluride, which has a ZT value ranging from 1 to 1.5).[11] More recently, an analytical model of a STEG using a heat pipe (HP) solar collector was reported by He et al.[12] A maximum power conversion efficiency of 3.346% was predicted for 1000 W/m^2 solar insolation.

Interest in STEGs is increasing, as explained above, but recent work has focused more on optimization of TE devices, e.g., searching for high-ZT materials,[13] optimizing the design of the TE module structure,[14] carrying out thermodynamic analysis of the TE generator,[15,16] and theoretical analysis of the performance of a single unit using a flat panel[9,11] as the solar collector, or an evacuated double-skin glass tube on the laboratory scale.[12] Very few reports analyze the efficiency of new solar thermoelectric cogenerator (STCG) systems, which provide both electricity and thermal energy (solar cogeneration), based on solar engineering concepts. A parabolic trough concentrator (PTC) combined with an evacuated tubular solar collector is a well-known configuration in current STPG systems. In an attempt to increase the feasibility of STCGs, we have designed a new STCG installation, in which the hot side of the TEM is tightly bonded to the rear side of the SSA fin which faces the PTC through the half-cylindrical part of the evacuated tube fixed at the focal line of the PTC, while the cold side of the TEM is tightly bonded to the heat sink which faces the sky through another half-cylindrical part of the evacuated tube. The idea behind solar cogeneration is to increase the total solar utilization efficiency up to 60% to 70% compared with the case of single generation of either electricity or thermal energy (30% to 40% under normal solar insolation and environmental thermoconditions). The additional distinguishing features of the new installation are that it can be used on a small and/or compact scale for distribution systems in remote areas, being mostly free from the weak points described above for the conventional STPG system. In particular, long operation hours and stable output can be achieved by using auxiliary waste heat supplies from industrial plants, power stations, and even scavenged waste heat from homes. Its ability to use a solar spectrum range covering the ultraviolet–visible–near infrared (UV–VIS-NIR) is also attractive from the solar engineering point of view.

It is important to study how the thermal losses affect the system efficiency when establishing a high-performance STEG system. Thermal engineering analysis for the present system is more complicated than for a solar collector on its own because the added TEM generates Joule heat during operation. This is taken into account in the present study.

We present details of the overall heat loss coefficients U_L from the SSA (most high-temperature component) to the surroundings (at ambient air temperature T_{amb}) and the sky (at temperature T_{sky}) for the present system as shown in Fig. 1. U_L is decomposed into the radiative heat transfer from the SSA to the evacuated tubular glass (ETG), etc., which is described in more detail in Sect. 2.3.

The feasibility of using the present STEG for cogeneration is thus confirmed. The conversion efficiency can reach 3.87% under 1000 W/m^2 solar insolation when a commercial TE module (ZT = 1) is used, and the solar thermal conversion efficiency exceeds 69%.

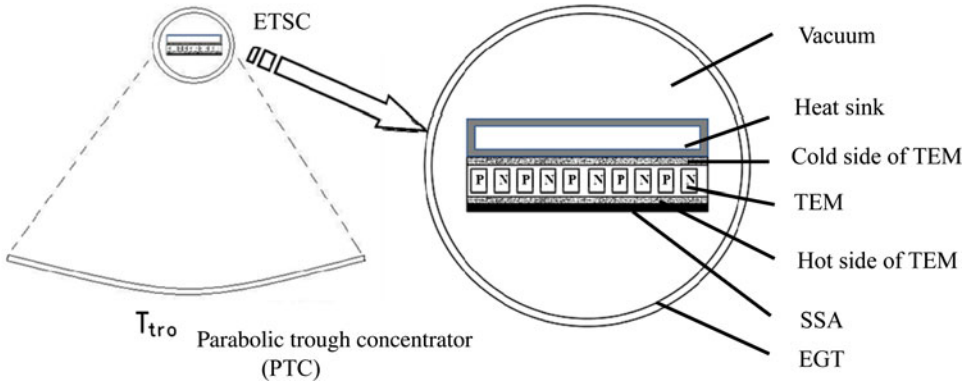

Fig. 1. Schematic of the newly designed cogeneration STEG. An evacuated tubular glass (ETG) with diameter D = 0.12 m and length L = 5.6 m is installed along the focal axis of the PTC. The right-hand side shows a magnified view of the evacuated tubular solar collector cross-section, in which the TEM is bonded to the SSA installed in the ETSC.

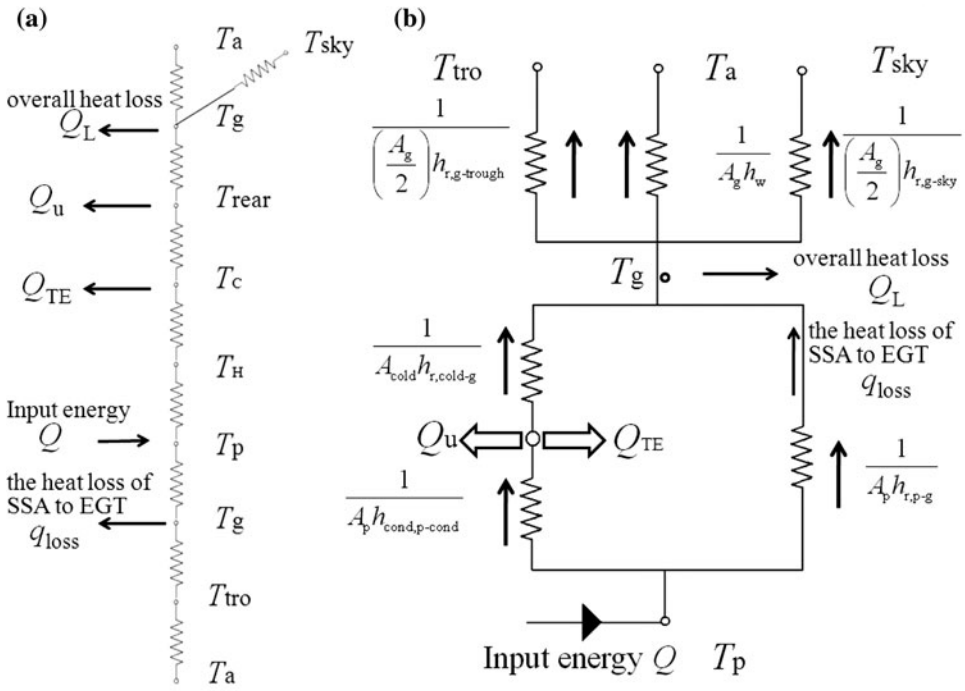

Fig. 2. (a) Single-temperature-node model for the system thermal analysis. (b) Overall equivalent thermal network of the system.

SIMULATION OF OVERALL SYSTEM EFFICIENCY

Solar Thermal Conversion Efficiency

We present the results of a solar thermal simulation based on energy balance and heat transfer that allows us to predict system efficiency. Following the well-known method used in solar thermal engineering,[17] we assume the single-node temperature model, which represents the average temperature of the respective component (or module) of the system shown in Fig. 2. The representative parameters used here are: the mean temperature of component y, T_y; the projection area of component y, A_y; the radiative heat transfer coefficient between components x and z, $h_{r,x-z}$; the conductive heat transfer coefficient from the SSA to the TEM, $h_{\text{cond,p-cond}}$; the heat transfer coefficient between the glass tube and the surroundings by forced wind convection (called the wind coefficient), h_w; and the emittance of component y, ε_y.

The *ad hoc* assumptions applied are: (a) the solar insolation I (W/m^2) impinging onto the aperture of the PTC of area A_{trough} is reflected by the PTC mirror (reflectance ρ = 0.95) and transmitted through the ETG (transmittance τ = 0.91), finally being absorbed at the solar selective absorber (SSA), which has high solar absorbance (α = 0.93) and low

emittance (ε = 0.2) for long-wave radiation (with width D = 0.06 m and length L = 5.6 m), being $IA_{\text{trough}}\rho\tau\alpha$, while the maximum temperature is reached at the SSA (T_{p}) in the system; (b) absorption of solar insolation by both the mirror and the ETG is negligibly small; (c) the lower half-cylinder of the ETG faces the mirror, and the upper half-cylinder faces the sky; (d) heat resistance between the SSA and the hot side of the TEM (with figure of merit Z and thermal conductance κ) is negligibly small, where $T_{\text{TEM,hot}}$ is represented by T_{p} to a good approximation; (e) the cold side of the TEM is closely bonded to the heat sink, and is always cooled down by the forced circulation coolant. Consequently, the temperature difference between the hot and cold sides of the TEM is kept in the range from 127 K to 177 K; (f) the heat resistance between the rear side and the surface side of the designated heat sink is negligibly small, so that to a good approximation $T_{\text{TEM,cold}} = T_{\text{HTS,surface}} = T_{\text{HTS,rear}}$ (represented by T_{c} hereafter); (g) the upper half-cylinder of the ETG is cooled down by the forced wind convection (with velocity v, assigned *ad hoc* an average wind speed of 1.3 m/s) at ambient air temperature (T_{a}), and radiative heat transfer occurs in the direction of the sky.

In Fig. 2, the respective temperature node is connected to the appropriate heat resistance (written using the reverse formula of the designated heat transfer coefficients) for the simulation using a conventional thermal network. Some portion of the collected solar thermal energy at the SSA (represented by Q) is used both for TEM generation (Q_{TE}) and as useful thermal energy (Q_{u}) converted by the circulated coolant, and the residual energy defined as $Q - (Q_{\text{TE}} + Q_{\text{u}})$ is finally dissipated to the sky with temperature T_{sky} and/or the surroundings with ambient air temperature T_{a} through both radiative heat transfer and wind heat transfer as overall heat loss (Q_{L}). The resultant thermal network between the SSA and the surroundings represented by ambient air or the sky is simplified as shown in the magnified view in Fig. 2 under the above *ad hoc* assumptions.

The solar thermal conversion efficiency η is defined as the ratio between the total useful energy Q_{therm} ($Q_{\text{therm}} = Q_{\text{TE}} + Q_{\text{u}}$) and the total solar energy impinging on the PTC aperture, which can be rewritten as

$$\eta \equiv (Q_{\text{u}} + Q_{\text{TE}})/IA_{\text{trough}} \equiv (Q - Q_{\text{L}})/IA_{\text{trough}}, \quad (1a)$$

$$\begin{aligned}\eta &= \rho\tau\alpha - U_{\text{L}}A_{\text{p}}(T_{\text{p}} - T_{\text{a}})/(A_{\text{trough}}I) \\ &= \eta_{\text{opt}} - U_{\text{L}}(T_{\text{p}} - T_{\text{a}})/(IC),\end{aligned} \quad (1b)$$

$$\eta_{\text{opt}} \equiv \rho\tau\alpha, \quad (1c)$$

where U_{L} is the overall heat loss coefficient from the SSA to the surroundings, η_{opt} is the optical efficiency, and C is the concentration ratio ($= A_{\text{trough}}/A_{\text{p}}$), by consideration of the heat flows in Fig. 2b following energy conservation. Equation 1b can be rewritten in another form as

$$\eta = \eta_{\text{opt}} - F'U'_{\text{L}}(T_{\text{g}} - T_{\text{amb}})/(IC), \quad (1d)$$

$$U'_{\text{L}} \equiv h_{\text{w}} + h_{\text{r,g-trough}} + h_{\text{r,g-amb}}, \quad (1e)$$

where $F' \equiv (A_{\text{g}}/2A_{\text{p}})$.

The Thermal-to-Electrical Conversion Efficiency of the TEM

The thermal-to-electrical conversion efficiency of a TEM can be expressed as[8]

$$\eta_{\text{TE}} = \frac{(T_{\text{H}} - T_{\text{C}})\left(\sqrt{1 + ZT_{\text{M}}} - 1\right)}{T_{\text{H}}\left(\sqrt{1 + ZT_{\text{M}}} + T_{\text{C}}/T_{\text{H}}\right)} \quad (2)$$

where T_{M} is the mean temperature of the hot and cold sides of the TEM, i.e., $T_{\text{M}} = \frac{T_{\text{H}}+T_{\text{C}}}{2}$. In this expression, the Joule heat generated in the TEM has been taken into account.[6]

In the simulations, we used two typical values of $T_{\text{TE,cold}}$, namely 323 K and 373 K, with two $ZT_{\text{TE,av}}$ values of 1 and 0.64, respectively, while the hot side of the TEM was fixed at 500 K as given in Table I. The obtained η_{TE} values are also listed in Table I.

Thermal Losses

Formulas for the heat transfer coefficient required in Fig. 2b were obtained by straightforward modification of the appropriate formulas in a standard solar engineering textbook[17] as follows:

(a) The radiative heat transfer coefficient between the SSA and the ETG is given by

$$h_{\text{r,p-g}} = \frac{\sigma\left(T_{\text{p}}^2 + T_{\text{g}}^2\right)(T_{\text{p}} + T_{\text{g}})}{\frac{1}{\varepsilon_{\text{p}}} + \frac{1}{\varepsilon_{\text{g}}} - 1}, \quad (3)$$

where σ is the Stefan–Boltzmann constant ($= 5.76 \times 10^{-8}$ W/m^2 K^4).

(b) The radiative heat transfer coefficient between the rear surface of the heat sink for coolant circulation and the ETG, $h_{\text{r,rear-g}}$, is obtained from a similar formula to Eq. 3 with T_{p} and ε_{p}

Table I. Thermal-to-electrical power conversion efficiency of a TEM

T_{C} (K)	T_{H} (K)	ZT_{M}	η_{TE} (%)
323	500	1	7.12
323	500	0.64	5.16
373	500	1	4.87
373	500	0.64	3.52

replaced with T_{rear} (=$T_{coolant}$) and ε_{rear}, respectively;

(c) The radiative heat transfer coefficient between the ETG and the mirror of the PTC, $h_{r,g-trough}$, is also obtained from a similar formula to Eq. 3 by substituting T_p and ε_p for T_{trough} (=T_{amb}) and ε_{trough} $(1 - \rho = 0.05)$, respectively;

(d) The radiative heat transfer coefficient between the ETG and the atmosphere is given by

$$h_{r,g-sky} = \sigma\varepsilon_g\left(T_g^2 + T_{sky}^2\right)\left(T_g + T_{sky}\right). \quad (4)$$

(e) The wind heat transfer coefficient is given by McAdams' empirical formula[17] as

$$h_w = 5.7 + 3.8v. \quad (5)$$

From Eqs. 1a and 1b, the total solar energy (Q) absorbed on the SSA is given by

$$\begin{aligned} Q &\equiv IA_{trough}\rho\tau\alpha \equiv IA_{trough}\eta_{opt} = I\eta_{opt}A_pC \\ &\equiv I\eta_{opt}(d \times L)C. \end{aligned} \quad (6)$$

From the appropriate mechanism for thermal-to-electricity conversion, the inner heat generated by TE, Q_{TE}, is given by

$$Q_{TE} = SIT_H + K(T_H - T_C) - \frac{1}{2}I^2R, \quad (7)$$

where the right-hand side terms in Eq. 7 correspond to Peltier heat, thermal conduction, and Joule heat. It is difficult to obtain Q_{TE} from Eq. 7 because the Peltier heat, thermal conduction, and Joule heat are complex in a TEM. The heat energy absorbed at the hot junction, Q_{TE}, is supplied by the solar energy (Q) absorbed on the SSA. Therefore, the heat energy absorbed at the hot junction, Q_{TE}, can also be given by $Q_{TE} = Q - q_{loss}$, where q_{loss} is the heat loss from the SSA to ETG, $q_{loss} = Ldh_{r,p-g}(T_p - T_g)$. Therefore,

$$Q_{TE} = Q - Ldh_{r,p-g}(T_p - T_g). \quad (8)$$

The total useful energy can be determined by calculation of the thermal flow based on the thermal network shown in Fig. 2b according to

$$\begin{aligned} Q_{therm} = {} & ILdC\eta_{opt} - \frac{A_g}{2}h_{r,g-trough}\left(T_g - T_{tro}\right) \\ & - \frac{A_g}{2}h_{r,g-sky}\left(T_g - T_{sky}\right) - A_gh_w\left(T_g - T_a\right). \end{aligned} \quad (9)$$

Therefore, the electrical conversion efficiency of the system is simply given by

$$\eta_{ele} \equiv \frac{Q_{ele}}{ILdC} = \frac{Q_{TE}\eta_{TE}}{ILdC}, \quad (10)$$

where Q_{ele} is the thermal energy for electricity generation.

The solar thermal conversion efficiency is given by

$$\eta_{solar} = \frac{Q_{therm}}{ILdC}. \quad (11)$$

When the hot side of the TEM is bonded closely to the SSA, the approximation $T_H = T_p$ is valid. In this case the temperature of the cold side of the TEM is taken as $T_C = T_{rear}$, T_c being the coolant temperature averaged over the tube inlet and the tube outlet. As the functional forms in Eqs. 3, 4, 8, and 9 do not contain linear relations between the designated temperatures, we calculated the appropriate values for the designated radiative heat transfer coefficient and wind heat transfer coefficient until sufficient numerical convergence had been obtained. The optimal results are given in Table II under the *ad hoc* assumption that the optimal values are T_g = 350 K, T_p = 500 K, T_{rear} = 373 K, ε_p = 0.2, ε_g = 0.8, ε_{rear} = 0.2, and ε_{tro} = 0.1.

SIMULATION RESULTS AND DISCUSSION

Figure 3 shows the concentration ratio (C) dependency of the electrical conversion efficiency of the designed STCG system for three different solar insolation values of 1000 W/m^2, 800 W/m^2, and 600 W/m^2. These correspond to good, common, and yearly averaged Guangzhou data cases, respectively. The conversion efficiency of solar energy into electricity (as defined in Eq. 10) increases with increasing figure of merit ZT_M of the TEM as shown in Fig. 3a, b. When the concentration ratio is low, the efficiency increases rapidly with increasing C in both cases, but after C reaches a certain value, the efficiency becomes constant.

To generate stable electricity, the temperature difference between the hot and cold sides of the TEM needs to be constant. The thermal losses are nearly constant for the designed STCG system as expressed by Q_L. Therefore, it is necessary that the waste heat module be exposed to a heat source at night or under poor solar insolation.

Thermal energy is another supply form for the STCG system. The dependence of the solar-to-thermal conversion efficiency on the concentration ratio is plotted in Fig. 4. To enhance solar to thermal energy conversion, a larger concentration ratio of up to 100 might be favorable if cost performance is not

Table II. Optimal values of the designated radiative heat transfer coefficient and wind coefficient

$h_{r,p-g}$	3.42 W/(m^2 K)
$h_{r,rear-g}$	2.04 W/(m^2 K)
$h_{r,g-trough}$	0.84 W/(m^2 K)
$h_{r,g-sky}$	5.92 W/(m^2 K)
h_w	10.62 W/(m^2 K)

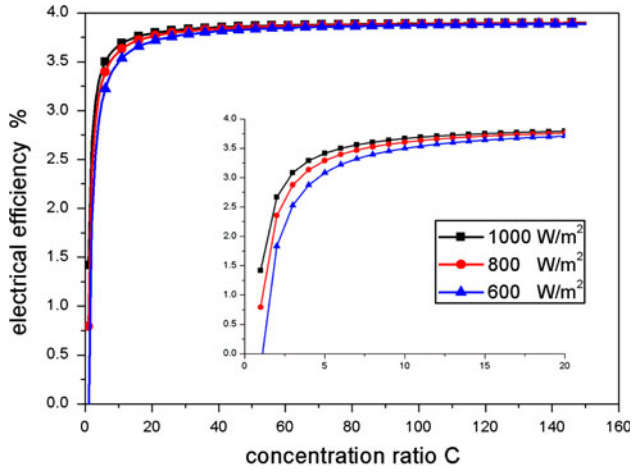

(a) ZT_M=1

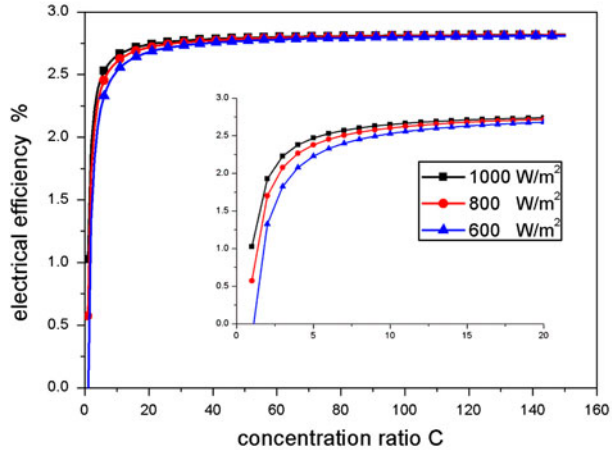

(b) ZT_M=0.64

Fig. 3. Efficiency of converting solar energy into electricity versus concentration ratio C for two different figures of merit ZT_M of TEM: (a) ZT_M = 1 and (b) ZT_M = 0.64. Saturation of the efficiency curve at low C is apparent in the inset.

an issue. However, for conversion of solar energy into electricity by the TEM as shown in Fig. 3, a larger concentration ratio is not feasible. To represent a balance between conversion to electricity and thermal energy, we set $C = 50$ for the present experimental system.

When the solar insolation, C value, and ZT_M are 1000 W/m^2, 50, and 1, respectively, the electrical conversion efficiency of the TE can reach 3.87%, assuming that the solar efficiency is about 69% at the absorber temperature of 500 K, the ambient temperature is 293 K, the ETG temperature is 350 K, and the rear surface of the TE has a temperature of 373 K by use of the forced circulation coolant, being the optimal values in the simulation.

The maximum solar-to-electricity conversion efficiency is 3.87% when the solar insolation, C value, and ZT_M are 1000 W/m^2, 50, and 1, respectively, as shown in Fig. 3a. Although the conversion efficiency is about 7.12% for the TEM at a temperature

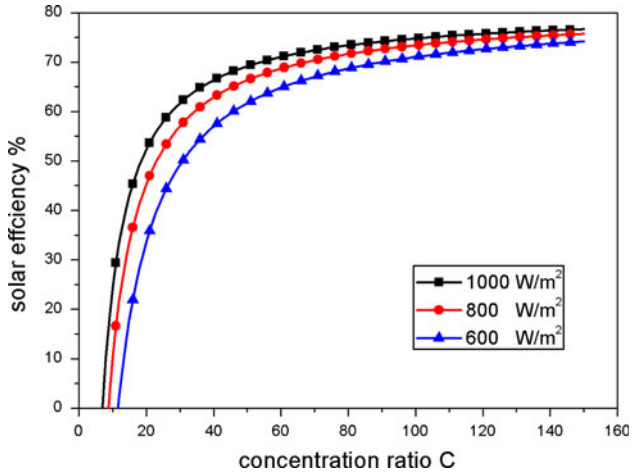

Fig. 4. Efficiency of converting solar into thermal energy versus concentration ratio C.

difference of 177 K, as listed in Table I, according to the simulation the system efficiency decreases greatly due to the overall thermal loss. Solar thermal engineering analysis and subsequent system design are thus very important for increasing the system efficiency, and studying how the thermal losses affect the system efficiency is helpful for establishing a high-performance STEG system for solar cogeneration purposes.

We propose a solar cogeneration system due to the low efficiency of thermal-to-electrical energy conversion (<10%) of the present TEM. About 69% of the solar energy can be converted into thermal energy. With an efficiency of 3.87% for the TEM, surplus solar thermal energy is needed to enhance the total solar energy utilization of this system. There are three feasible technologies for achieving this. Hot water utilization is a simple and common way. The second way is installation of an auxiliary gas-turbine-type electric generator using a low-boiling-point fluid for high-pressure gas production. The third one is hydrogen production installed utilizing a thermal decomposition chemical reaction at a reasonably low temperature such as a solar thermal cell reaction. Although the details of this will appear elsewhere, the feasibility of using pentane (C_5H_{12}), which has a boiling point of 36.1°C, and 2-propanol [$CH_3CH(OH)CH_3$], which has a decomposition temperature of 82°C to 83°C, has been confirmed previously by one of the authors (T.T.) using a solar thermal process.[18,19] Both candidate solvents have sufficiently low boiling and/or decomposition point for use as the surplus solar thermal energy source in the new system.

CONCLUSIONS

We confirm the feasibility of using a solar thermoelectric cogeneration system with a TEM installed in an evacuated tubular collector with parabolic trough concentrator. When the solar

insolation, concentration ratio, and ZT_M are 1000 W/m^2, 50, and 1, respectively, the solar-to-thermal conversion efficiency is 69% and the solar-to-electrical conversion efficiency can reach 3.87% when a forced circulation coolant is used with the TEM. To enhance the total solar energy utilization of this system, we briefly outline three new additional subsystems for providing hot water, auxiliary electricity from gas turbines, and/or hydrogen production using a solar thermal cell.

ACKNOWLEDGEMENTS

This work was supported by the Guangdong Natural Science Foundation, Grant No. 915100700 6000009; Guangdong Provincial Science and Technology Grant No. 2011B010100043 and Chinese Academy of Sciences: Key Laboratory of Renewable Energy and Natural Gas Hydrate Foundation, Grant No. y107j3.

REFERENCES

1. M. Telkes, *J. Appl. Phys.* 25, 765 (1954).
2. R. Venkatasubramanian, E. Siivola, T. Colpitts, and B. O'Quinn, *Nature* 413, 597 (2001).
3. T.C. Harman, P.J. Taylor, M.P. Walsh, and B.E. LaForge, *Science* 297, 2229 (2002).
4. K.F. Hsu, S. Loo, F. Guo, W. Chen, J.S. Dyck, C. Uher, T. Hogan, E.K. Polychroniadis, and M.G. Kanatzidis, *Science* 303, 818 (2004).
5. C.B. Vining, *Nat. Mater.* 8, 83 (2009).
6. D.M. Rowe, *Thermoelectrics Handbook Nano to Macro* (Boca Raton: CRC Taylor & Francis, 2006).
7. J.H. Yang and F.R. Stabler, *J. Electron. Mater.* 38, 1245 (2009).
8. L. Bell, *Science* 321, 1457 (2008).
9. D. Kraemer, B. Poudel, H.P. Feng, J.C. Caylor, B. Yu, X. Yan, Y. Ma, X.W. Wang, D.Z. Wang, A. Muto, K. McEnaney, M. Chiesa, Z.F. Ren, and G. Chen, *Nat. Mater.* 10, 532 (2011).
10. J. Karni, *Nat. Mater.* 10, 481 (2011).
11. K. McEnaney, D. Kraemer, Z.F. Ren, and G. Chen, *J. Appl. Phys.* 110, 074502 (2011).
12. W. He, Y.H. Su, S.B. Riffat, J.X. Hou, and J. Ji, *Appl. Energy* 88, 5083 (2011).
13. H. Scherrer, L. Vikhor, B. Lenoir, A. Dauscher, and P. Poinas, *J. Power Sources* 115, 141 (2003).
14. S.A. Omer and D.G. Infield, *Solar Energy Mater. Solar Cells* 53, 67 (1998).
15. J.C. Chen, *J. Appl. Phys.* 79, 5–2717 (1996).
16. R. Amatya and R.J. Ram, *J. Electron. Mater.* 39, 1735 (2010).
17. J.A. Duffie and W.A. Beckman, *Solar Energy Thermal Processes*, chap. 7: Flat Plate Collector & chap. 8: Focusing Collector (New York, NY: Wiley, 1974), pp. 120–214.
18. T. Tanaka, *Eco Ind.* 5, 5 (1999).
19. Y. Ando and T. Tanaka, *Jpn. J. Solar Energy* 28, 40 (2002).